Activation cross-sections of titanium isotopes at neutron energies of 13.5–14.8 MeV*

Fengqun Zhou(周丰群)[1,2] Yueli Song(宋月丽)[2] Yong Li(李勇)[2] Xiaojun Sun(孙小军)[2] Shuqing Yuan(袁书卿)[2;1)]

[1]Henan Key Laboratory of Research for Central Plains Ancient Ceramics, Pingdingshan University, Pingdingshan 467000, China
[2]School of Electrical and Mechanical Engineering, Pingdingshan University, Pingdingshan 467000, China

Abstract: The cross-sections for ^{46}Ti(n,2n)^{45}Ti, ^{46}Ti(n,p)$^{46m+g}$Sc+^{47}Ti(n,d*)$^{46m+g}$Sc, ^{46}Ti(n,p)$^{46m+g}$Sc, ^{47}Ti(n,p)^{47}Sc+^{48}Ti(n,d*)^{47}Sc, ^{47}Ti(n,p)^{47}Sc, ^{48}Ti(n,p)^{48}Sc+^{49}Ti(n,d*)^{48}Sc,^{48}Ti(n,p)^{48}Sc, and ^{50}Ti(n,α)^{47}Ca reactions were investigated around neutron energies of 13.5–14.8 MeV by means of the activation technique. Fast neutrons were produced by the ^{3}H(d,n)^{4}He reaction. Neutron energies from different directions in the measurements were obtained in advance using the method of cross-section ratios for ^{90}Zr(n,2n)$^{89m+g}$Zr and ^{93}Nb(n,2n)^{92m}Nb reactions. The results obtained are analyzed and compared with the experimental data provided by the literature and verified nuclear data in the JEFF-3.3, CENDL-3.1, ENDF/B-VIII.0 libraries, as well as results calculated by Talys-1.9 code.

Keywords: titanium, neutron reaction cross section, D-T neutron, activation technique

PACS: 25.40.-h, 28.20.-v, 24.60.Dr **DOI:** 10.1088/1674-1137/43/9/094001

1 Introduction

Accurate and reliable neutron induced cross-sections of titanium isotopes around the neutron energy of 14 MeV are important for fusion reactor design and related nuclear engineering calculations, as titanium is a vital structural component in the fusion reactor. These cross-sections can reflect the interactional mechanism between target nucleus and incident particles, and provide us with a deep understanding of the nuclear force and structure of titanium. Activation cross-sections of (n,2n), (n,p), and (n,α) reactions of titanium isotopes around the neutron energy of 14 MeV have been measured by many researchers, and they can be found in experimental nuclear reaction data (EXFOR) [1]. The majority of these measurements were acquired before the 1980s, and large discrepancies exist in those data. Moreover, discrepancies exist in the results of different researchers acquired after the 1980s. Thus, it is necessary to conduct the measurements again and more accurately. In the present work, the cross-sections for the ^{46}Ti(n,2n)^{45}Ti,^{46}Ti(n,p)$^{46m+g}$Sc+^{47}Ti(n,d*)$^{46m+g}$Sc[(n,d*)=(n,d)+(n,n+p)],^{46}Ti(n,p)$^{46m+g}$Sc, ^{47}Ti(n,p)^{47}Sc+^{48}Ti(n,d*)^{47}Sc,^{47}Ti(n,p)^{47}Sc,^{48}Ti(n,p)^{48}Sc+^{49}Ti(n,d*)^{48}Sc, ^{48}Ti(n,p)^{48}Sc, and ^{50}Ti(n,α)^{47}Ca reactions have been measured in the neutron energy range of 13.5–14.8 MeV with a gamma-ray counting technique using a high-resolution gamma-ray spectrometer and data acquisition system. Pure titanium foils were used as the target material. The reaction yields were obtained by absolute measurement of the gamma activities of the product nuclei using a coaxial high-purity germanium detector. The results measured are compared with past data and with the data verified, as well as the theoretical results.

2 Experimental details and data analysis

Nuclear reaction cross-sections were obtained by means of activation and identification of the radioactive products. Details were described in numerous publications [2–5]. Here only some salient features are presented that are relevant to present measurements.

Natural titanium foils, whose purity and thickness are 99.99% and 2.98 –3.0 mm, respectively, were used to make circular samples with a diameter of 20 mm. They each were placed between thin niobium disks of the same diameter of 20 mm, whose purity is 99.99% and thickness is 1 mm.

Irradiation of the samples was carried out at the K-400 Neutron Generator at the Institute of Nuclear Phys-

Received 26 March 2019, Published online 17 July 2019

* Supported by the National Natural Science Foundation of China (11575090, 11605099)

1) E-mail: yuansq2017@163.com

ics and Chemistry, China Academy of Engineering Physics. Samples were irradiated for 3–7.5 h. The neutrons in the 14 MeV region with a yield of 4×10^{10} n/s to 5×10^{10} n/s were produced by the ^{3}H(d,n)^{4}He reaction with a deuteron beam energy of 255 keV and a beam current of 350 μA. The solid tritium–titanium target used in the generator was about 2.19 mg/cm^2 thick. During the irradiation, the neutron flux was monitored by the accompanying α-particles, which were measured with a Au–Si surface barrier detector used in the 135° accompanying a-particle tube, so that corrections could be made for the small fluctuations in the neutron flux. Groups of samples were placed at angles of 0°, 45°, 90°, and 135° respectively, which are relative to the direction of the deuteron beam and centered about the T–Ti target at a distance of 3–5 cm. The neutron energies in the measurements were determined in advance by cross-section ratios for the ^{90}Zr(n,2n)$^{89m+g}$Zr and ^{93}Nb(n,2n)^{92m}Nb reactions [6]. The measured neutron energies were 13.5 ± 0.2, 14.1 ± 0.2, 14.4 ± 0.2, and 14.8±0.2 MeV at the irradiation positions of 0°, 45°, 90°, and 135° angles relative to the beam direction, respectively.

After irradiation, the samples were cooled for 28 minutes to 87 hours. The activities of ^{45}Ti, $^{46m+g}$Sc, ^{47}Sc, ^{48}Sc, ^{47}Ca, and ^{92m}Nb were measured by a well-calibrated GEM-60P coaxial high-purity germanium (HPGe) detector (crystal diameter 70.1 mm, crystal length 72.3 mm) with a relative efficiency of ~68% and an energy resolution of ~1.69 keV FWHM at 1.33 MeV for ^{60}Co. The samples were measured for 1.5–9.5 h. The efficiency of the detector was pre-calibrated using various standard γ sources. Figure 1 and Fig. 2 show part of the γ-ray spectrum acquired from the titanium samples after a cooling time of about 53 min and 78.73 h, respectively.

The associated decay data of all the activation products and the natural abundance of target isotopes under investigation are summarized in Table 1[7]. The abundance of ^{93}Nb comes from Ref. [8], as no abundance of ^{93}Nb is given in Ref. [7].

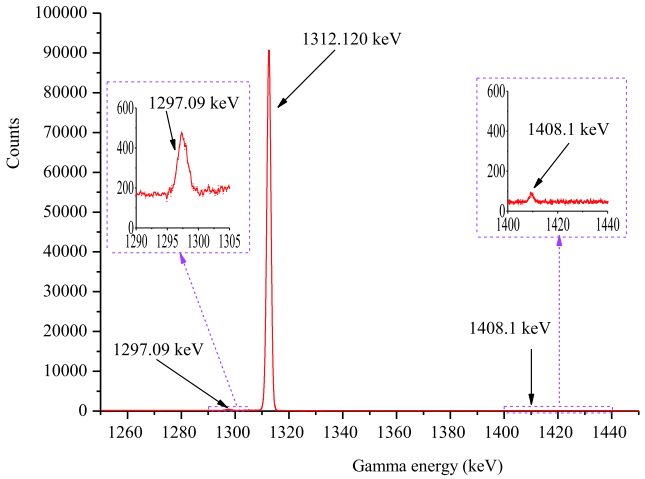

Fig. 1. (color online) Part of γ-ray spectrum of titanium about 53 m after the end of irradiation.

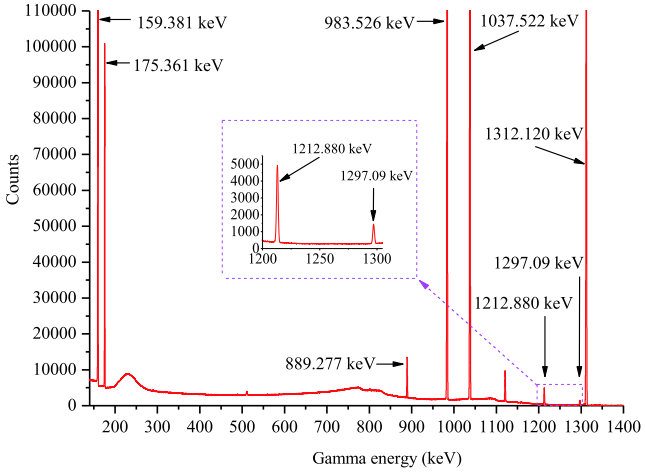

Fig. 2. (color online) Part of γ-ray spectrum of titanium about 78.73 h after the end of irradiation.

We calculated the measured cross-sections by means of the equation proposed by Kong et al.[9].

The cross-sections of the ^{46}Ti(n,2n)^{45}Ti, ^{46}Ti(n,p)$^{46m+g}$Sc + ^{47}Ti(n,d*)$^{46m+g}$Sc, ^{46}Ti(n,p)$^{46m+g}$Sc, ^{47}Ti(n,p)^{47}Sc + ^{48}Ti(n,d*)^{47}Sc, ^{47}Ti(n,p)^{47}Sc, ^{48}Ti(n,p)^{48}Sc + ^{49}Ti(n,d*)^{48}Sc, ^{48}Ti(n,p)^{48}Sc, and ^{50}Ti(n,α)^{47}Ca reactions were acquired relative to those of the ^{93}Nb(n,2n)^{92m}Nb reaction. The cross-section values of the monitor reaction ^{93}Nb (n,2n) ^{92m}Nb were 457.9 ± 6.8, 459.8 ± 6.8, 459.8 ± 6.8 and 459.7 ± 5.0 mb at the neutron energies of 13.5, 14.1, 14.4, and 14.8 MeV, respectively[10]. The results obtained in this work are summarized in Tables 2-6 and plotted in Figs. 3– 10. The cross-sections of the ^{46}Ti(n,2n)^{45}Ti, ^{46}Ti(n,p)$^{46m+g}$Sc + ^{47}Ti(n,d*)$^{46m+g}$Sc, ^{46}Ti(n,p)$^{46m+g}$Sc, ^{47}Ti(n,p)^{47}Sc+ ^{48}Ti(n,d*)^{47}Sc, ^{47}Ti(n,p)^{47}Sc, ^{48}Ti(n,p)^{48}Sc+ ^{49}Ti(n,d*)^{48}Sc, ^{48}Ti(n,p)^{48}Sc, and ^{50}Ti(n,α)^{47}Ca reactions around 14 MeV neutron energy have been obtained by about 20, 6, 18, 4, 18, 3, 34, and 14 laboratories, respectively [1]. The previous measurements, whose results were published after 1980, are also summed up in Tables 2–6 and plotted in Figs. 3–10 for comparison. For these reactions mentioned above, their evaluation cross-section curves of JEFF-3.3, CENDL-3.1, ENDF/B-VIII.0 at neutron energies from the threshold to 20 MeV are plotted in Figs. 3-10 for comparison. The theoretical calculation cross-section data at different neutron energies from the threshold to 20 MeV were calculated via the computer code system Talys-1.9 [11–14]. Default values of parameters are adopted in the calculation. The theoretical calculation values at the neutron energies of 13.5, 14.1, 14.4, and 14.8 MeV are also summarized in Tables 2–6 and the theoretical calculation curves plotted in Figs.

3-10 for comparison.

The complete description of TALYS can be found in the Talys-1.9 manual [11]. TALYS is a computer code system built for the analysis and prediction of nuclear reactions based on physics models and parameterizations [11-13]. It is a versatile tool for the analyses of basic microscopic scientific experiments or for generation of nuclear data for applications. It can simulate nuclear reactions involving neutrons, photons, protons, deuterons, tritons, ^{3}He, and α-particles in the 0.001–200 MeV energy range and for target nuclides of mass of 12 and heavier. To deal with the neutron induced nuclear reactions, we use the optical model. All optical model calculations are performed by ECIS-06 [14], which is implanted as a subroutine in Talys.

The cross-sections of the ^{46}Ti(n,p)$^{46m+g}$Sc + ^{47}Ti(n,d*)$^{46m+g}$Sc reaction were calculated using the equation proposed by Kong et al. [9]. The abundance of the target isotope is equal to that of the first mentioned isotope. The contribution of the ^{48}Ti(n,t)$^{46m+g}$Sc reaction was neglected because of its tiny cross-section (10^{-7} mb). The cross-sections of the ^{46}Ti(n,p)$^{46m+g}$Sc reaction were com-

Table 1. Reactions and associated decay data of objective activation products.

reaction	abundance of target isotope (%)	half-life of product	E_γ /keV	I_γ (%)
^{46}Ti(n,2n)^{45}Ti	8.25	184.8 m	1408.1	0.085
^{46}Ti(n,p)$^{46m+g}$Sc + ^{47}Ti(n,d*)$^{46m+g}$Sc	8.25[a]	83.79 d	889.277	99.9840
^{46}Ti(n,p)$^{46m+g}$Sc	8.25	83.79 d	889.277	99.9840
^{47}Ti(n,p)^{47}Sc + ^{48}Ti(n,d*)^{47}Sc	7.44[a]	3.3492 d	159.381	68.3
^{47}Ti(n,p)^{47}Sc	7.44	3.3492 d	159.381	68.3
^{48}Ti(n,p)^{48}Sc + ^{49}Ti(n,d*)^{48}Sc	73.72[a]	43.67 h	1312.120	100
^{48}Ti(n,p)^{48}Sc	73.72	43.67 h	1312.120	100
^{50}Ti(n,α)^{47}Ca	5.18	4.536 d	1297.09	67
^{93}Nb(n,2n)^{92m}Nb	100[b]	10.15 d	934.44	99.15

[a]Abundance of target isotope is that of the first mentioned isotope for the ^{46}Ti(n,p)$^{46m+g}$Sc + ^{47}Ti(n,d*)$^{46m+g}$Sc, ^{47}Ti(n,p)^{47}Sc + ^{48}Ti(n,d*)^{47}Sc, and ^{48}Ti(n,p)^{48}Sc + ^{49}Ti(n,d*)^{48}Sc reactions. [b]We used the value given by Ref. [8].

Table 2. Summary of the cross section for the ^{46}Ti(n,2n)^{45}Ti reaction around 14 MeV neutron energy.

reaction	this work		literature values		
	E_n /MeV	σ /mb	E_n /MeV	σ /mb	reference
^{46}Ti(n,2n)^{45}Ti	14.1 ± 0.2	13.3 ± 1.0 (37.8[c])	14.7	47 ± 2	[15]
	14.4 ± 0.2	37.8 ± 2.8 (54.8[c])	14.7	47 ± 2	[16]
	14.8 ± 0.2	53.2 ± 3.2 (91.9[c])	13.63	0.182 ± 0.029	[17]
			13.73	0.894 ± 0.059	[17]
			14	8.77 ± 0.48	[17]
			14.47	28.9 ± 1.6	[17]
			14.72	42 ± 2.3	[17]
			15.01	54.9 ± 3	[17]
			14.6	51 ± 2	[18]
			14.8	33 ± 6.6	[19]
			13.5	2.2 ± 0.2	[20]
			13.77	7.5 ± 0.6	[20]
			14.1	17.7 ± 1.3	[20]
			14.39	30.9 ± 2.3	[20]
			14.66	42 ± 3.2	[20]
			14.78	50.2 ± 3.8	[20]

[c] Theoretical calculation cross-section data obtained from Talys-1.9.

Table 3. Summary of cross sections for ^{46}Ti(n,p)$^{46m+g}$Sc+^{47}Ti(n,d*)$^{46m+g}$Sc and ^{46}Ti(n,p)$^{46m+g}$Sc reactions around 14 MeV neutron energy.

reaction	this work		literature values		
	E_n /MeV	σ /mb	E_n /MeV	σ /mb	reference
^{46}Ti(n,p)$^{46m+g}$Sc + ^{47}Ti(n,d*)$^{46m+g}$Sc	13.5 ± 0.2	289.9 ± 15.1 (212.9 c)	13.447	289.3 ± 10.3	[21]
	14.1 ± 0.2	280.6 ± 11.8 (234.3 c)	13.921	296.2 ± 10.7	[21]
	14.4 ± 0.2	262.4 ± 11.9 (244.0 c)	14.126	286.8 ± 13.5	[21]
	14.8 ± 0.2	251.1 ± 10.6 (255.8 c)	14.347	287.3 ± 11.2	[21]
			14.921	292.6 ± 10.9	[21]
			14.7	311 ± 7.5	[22]
			13.5	306 ± 15	[23]
			13.84	286 ± 14	[23]
			14.18	299 ± 13	[23]
			14.38	305 ± 13	[23]
			14.67	294 ± 12	[23]
			14.81	305 ± 12	[23]
			13.39	305 ± 18	[24]
			13.43	312 ± 19	[24]
			14.36	299 ± 18	[24]
			14.39	294 ± 18	[24]
			14.7	304 ± 10	[25]
^{46}Ti(n,p)$^{46m+g}$Sc	13.5 ± 0.2	275.1 ± 14.4 (183.6[c])	13.33	274 ± 14	[17]
	14.1 ± 0.2	247.8 ± 10.5 (180.9[c])	13.56	264 ± 14	[17]
	14.4 ± 0.2	218.2 ± 9.9 (163.6[c])	13.98	253 ± 13	[17]
	14.8 ± 0.2	192.1 ± 8.1 (157.0[c])	14.42	240 ± 12	[17]
			14.65	234 ± 13	[17]
			14.91	210 ± 14	[17]
			14.7	261 ± 27	[26]
			13.77	302 ± 33	[27]
			13.93	291 ± 38	[27]
			14.11	302 ± 33	[27]
			14.3	298 ± 34	[27]
			14.73	298 ± 34	[27]
			14.83	267 ± 39	[27]
			14.05	267.8 ± 9.3	[28]
			13.68	282 ± 13.9	[29]
			14.58	284.7 ± 14	[29]
			14.8	226.2 ± 22.4	[30]
			14.8	266.7 ± 3.2	[31]
			13.77	310 ± 33	[32]
			13.93	297 ± 38	[32]
			14.11	310 ± 33	[32]
			14.3	306 ± 37	[32]
			14.47	242 ± 33	[32]
			14.73	306 ± 34	[32]
			14.83	275 ± 39	[32]

[c] Theoretical calculation cross-section data obtained from Talys-1.9.

Table 4. Summary of cross-sections for ^{47}Ti(n,p)^{47}Sc+^{48}Ti(n,d*)^{47}Sc and ^{47}Ti(n,p)^{47}Sc reactions around 14 MeV neutron energy.

reaction	this work		literature values		
	E_n /MeV	σ /mb	E_n /MeV	σ /mb	reference
^{47}Ti(n,p)^{47}Sc + ^{48}Ti(n,d*)^{47}Sc	13.5 ± 0.2	169.3 ± 6.8 (274.2[c])	13.447	173.8 ± 4.9	[21]
	14.1 ± 0.2	197.6 ± 8.3 (262.3[c])	13.921	197.6 ± 5.7	[21]
	14.4 ± 0.2	228.0 ± 9.6 (244.3[c])	14.126	203.2 ± 5.9	[21]
	14.8 ± 0.2	259.6 ± 10.9 (241.2[c])	14.347	224.3 ± 6.8	[21]
			14.921	267.8 ± 8	[21]
			14.7	257 ± 12	[25]
			14.1	220 ± 5	[33]
+			13.75	164	[34]
			13.92	186	[34]
			14.11	186	[34]
			14.31	192	[34]
			14.49	218	[34]
			14.76	256	[34]
			14.86	271	[34]
^{47}Ti(n,p)^{47}Sc	13.5 ± 0.2	151.0 ± 6.1 (273.0[c])	13.33	144.5 ± 9.7	[17]
	14.1 ± 0.2	146.9 ± 6.2 (257.5[c])	13.56	143.9 ± 9.7	[17]
	14.4 ± 0.2	153.3 ± 6.5 (236.5[c])	13.98	135.5 ± 9.2	[17]
	14.8 ± 0.2	133.6 ± 5.7 (226.0[c])	14.42	130.5 ± 8.9	[17]
			14.65	127.1 ± 8.7	[17]
			14.91	121.5 ± 8.4	[17]
			14.7	151 ± 4	[26]
			14.73	142 ± 21	[27]
			14.83	131 ± 15	[27]
			14.6	174.5 ± 13.1	[30]
			14.8	169.5 ± 7.0	[31]
			14.0	103 ± 10	[35]
			14.3	158 ± 9	[36]
			14.9	142 ± 12	[36]
			14.8	103 ± 10	[37]

[c] Theoretical calculation cross-section data obtained from Talys-1.9.

Table 5. Summary of cross-sections for ^{48}Ti(n,p)^{48}Sc+^{49}Ti(n,d*)^{48}Sc and ^{48}Ti(n,p)^{48}Sc reactions around 14 MeV neutron energy.

reaction	this work		literature values		
	E_n /MeV	σ /mb	E_n /MeV	σ /mb	reference
^{48}Ti(n,p)^{48}Sc + ^{49}Ti(n,d*)^{48}Sc	13.5 ± 0.2	58.6 ± 2.5 (95.9[c])	14.7	68.7 ± 2.1	[25]
	14.1 ± 0.2	58.4 ± 2.5 (104.2[c])	14.8	73 ± 3.5	[38]
	14.4 ± 0.2	60.4 ± 2.6 (108.1[c])			
	14.8 ± 0.2	60.5 ± 2.5 (111.0[c])			
^{48}Ti(n,p)^{48}Sc	13.5 ± 0.2	58.6 ± 2.5 (95.1[c])	13.33	55.3 ± 2.6	[17]
	14.1 ± 0.2	58.2 ± 2.5 (102.1[c])	13.57	54.7 ± 2.6	[17]
	14.4 ± 0.2	60.2 ± 2.6 (104.4[c])	13.98	57.8 ± 2.8	[17]
	14.8 ± 0.2	60.1 ± 2.5 (104.2[c])	14.67	60.4 ± 2.9	[17]
			14.93	59.6 ± 2.9	[17]
			13.447	63.31 ± 2.23	[21]

Table 5 – continued from previous page

reaction	this work		literature values		
	E_n /MeV	σ /mb	E_n /MeV	σ /mb	reference
			13.921	67.18±2.54	[21]
			14.126	63.5±2.42	[21]
			14.347	67.75±2.71	[21]
			14.921	62.46±2.59	[21]
			13.5	61.3±2.8	[23]
			13.84	62.4±2.8	[23]
			14.18	64.4±2.7	[23]
			14.38	65.7±2.7	[23]
			14.67	63.5±2.6	[23]
			14.81	65.6±2.6	[23]
			14.7	76±2	[26]
			13.77	51±3	[27]
			13.99	53±3	[27]
			14.11	55±3	[27]
			14.3	55±3	[27]
			14.47	55±3	[27]
			14.73	60±3	[27]
			14.83	58±3	[27]
			14.05	58.6±1.8	[28]
			13.68	58.7±3.1	[29]
			14.36	61.3±3.4	[29]
			14.58	62.8±3.2	[29]
			14.77	63.4±3.7	[29]
			14.8	61.1±6.7	[30]
			14.8	71.7±2.7	[31]
			13.77	51±3	[32]
			13.93	53±3	[32]
			14.11	55±3	[32]
			14.3	53±3	[32]
			14.47	55±3	[32]
			14.73	61±3	[32]
			14.83	56±3	[32]
			14	68±2.6	[33]
			14.1	63±2	[33]
			14.0	60±4	[35]
			14.3	72±3	[36]
			14.9	69±6	[36]
			14.8	60±4	[37]
			14.6	67±4	[39]
			14.5	66	[40]
			14.66	69.4	[40]
			14.8	67.6	[40]
			14.85	67.5	[40]
			14.9	66.3	[40]
			14.8	60±5	[41]

[c] The theoretical calculation cross-section data by using the computer code system Talys-1.9.

Table 6. Summary of cross-section for ^{50}Ti(n,α)^{47}Ca reaction around 14 MeV neutron energy.

reaction	this work		literature values		
	E_n /MeV	σ /mb	E_n /MeV	σ /mb	reference
^{50}Ti(n,α)^{47}Ca	13.5 ± 0.2	5.75 ± 0.35 (2.01[c])	13.35	6.37 ± 0.62	[17]
	14.1 ± 0.2	7.94 ± 0.42 (2.51[c])	13.58	6.68 ± 0.46	[17]
	14.4 ± 0.2	8.46 ± 0.48 (2.97[c])	13.99	7.01 ± 0.7	[17]
	14.8 ± 0.2	9.47 ± 0.99 (3.53[c])	14.68	9.31 ± 0.78	[17]
			14.95	10.41 ± 0.88	[17]
			13.5	6.6 ± 0.5	[23]
			13.84	7.4 ± 0.5	[23]
			14.18	8 ± 0.5	[23]
			14.38	8.9 ± 0.5	[23]
			14.67	9.6 ± 0.5	[23]
			14.81	9.5 ± 0.6	[23]
			14.7	8.5 ± 0.5	[25]
			14.7	11 ± 2	[26]
			14.8	9 ± 0.8	[31]
			14.6	8.6 ± 0.6	[39]
			13.6	6.41 ± 0.68	[42]
			13.68	6.54 ± 0.72	[42]
			14.1	7.55 ± 0.73	[42]
			14.46	8.37 ± 0.75	[42]
			14.72	9.22 ± 0.61	[42]
			14.86	9.8 ± 0.98	[42]
			13.43	6.6 ± 0.5	[43]
			14.36	7.9±0.6	[43]

[c] Theoretical calculation cross-section data obtained from Talys-1.9.

puted using the equation proposed by Kong et al. [9], subtracting the contribution of the ^{47}Ti(n,d*)$^{46m+g}$Sc reaction with its evaluated values (16.20, 36.02, 48.40, and 64.61 mb at the neutron energies of 13.5, 14.1,14.4, and 14.8 MeV, respectively) from JEFF-3.3. We ignored the contribution of the ^{48}Ti(n,t)$^{46m+g}$Sc reaction due to its tiny cross-section (10^{-7} mb).

The cross-sections of the ^{47}Ti(n,p)^{47}Sc + ^{48}Ti(n,d*)^{47}Sc reaction were computed using the same method as above. The contribution from the ^{50}Ti(n,α)^{47}Ca→^{47}Sc decay was subtracted using a formula similar to the one used to reduce the influence of an excited state on the ground state in Ref. [44], and the contribution of the ^{49}Ti(n,t)^{47}Sc reaction was neglected due to its tiny cross-section (on the order of μb). The cross-sections of the ^{47}Ti(n,p)^{47}Sc reaction were computed through the equation proposed by Kong et al. [9] subtracting the contribution from the ^{50}Ti(n,α)^{47}Ca→^{47}Sc decay and the contribution of the ^{48}Ti(n,d*)^{47}Sc reaction with its evaluated values (1.84, 4.77, 7.46, and 12.28 mb at the neutron energies of 13.5, 14.1,14.4, and 14.8 MeV, respectively) from JEFF-3.3. We ignored the contribution of the ^{49}Ti(n,t)^{47}Sc reaction due to its tiny cross-section value (on the order of μb).

The cross-sections of the ^{48}Ti(n,p)^{48}Sc + ^{49}Ti(n,d*)^{48}Sc reaction were also calculated using the same method as above. The contribution of the ^{50}Ti(n,t)^{48}Sc reaction was neglected due to its tiny cross-section (10^{-9} mb). The cross-sections of the ^{48}Ti(n,p)^{48}Sc reaction were computed by equation proposed by Kong et al. [9], subtracting the contribution of the ^{49}Ti(n,d*)^{48}Sc reaction with its evaluated values (0.60, 1.67, 2.71, and 4.64 mb at the neutron energies of 13.5, 14.1, 14.4, and 14.8 MeV respectively) from JEFF-3.3. We overlooked the contribution of the ^{50}Ti(n,t)^{48}Sc reaction due to its tiny cross-section (10^{-9} mb).

3 Results and discussion

In this study, corrections were made concerning the

fluctuation of the neutron flux during the irradiation, γ-ray self-absorption in the sample, and the sample geometry. The uncertainties in our work mainly stem from counting statistics (0.5% –9.6%), standard cross-section uncertainties (1.1% –1.5%), detector efficiency (2.0%), weight of samples (0.1%), sample geometry (1.0%), self-absorption of γ-ray (1.0%), and fluctuation of the neutron flux (1.0%), etc.

For the ^{46}Ti(n,2n)^{45}Ti reaction, which is shown in Table 2 and Fig.3, there are small discrepancies in these verified values of JEFF-3.3, CENDL-3.1, and ENDF/B-VIII.0 around the neutron energy of 14 MeV, whereas the results obtained from Talys-1.9 are much higher than the above obtained and all experimental values. At 14.1 MeV neutron energy, our result is in agreement, within experimental error, with that of the excitation curve of Ikeda et al. [17] at the same energy, whereas it is lower than the verified values of JEFF-3.3,CENDL-3.1 and ENDF/B-VIII.0 at the corresponding energy. At 14.8 MeV neutron energy, our result is in agreement, within experimental error, with that of the excitation curve of Csikai [20] at the same energy as well as the verified values of CENDL-3.1 and ENDF/B-VIII.0 at the corresponding energy. At 14.4 MeV neutron energy, our result is between that of the verified values of JEFF-3.3, CENDL-3.1, and ENDF/B-VIII.0 and the theoretical calculation results.

For the ^{46}Ti(n,p)$^{46m+g}$Sc + ^{47}Ti(n,d*)$^{46m+g}$Sc reaction, we can see from Table 3 and Fig.4 that not only the trends of these excitation curves of JEFF-3.3, CENDL-3.1, ENDF/B-VIII.0 and the results calculated from Talys-1.9, but also the trends of some experimental excitation curves [21, 23, 24] are different around the neutron energy of 14 MeV. In addition, there are large discrepancies in these verified values of JEFF-3.3, CENDL-3.1 and ENDF/B-VIII.0 around the neutron energy of 14 MeV, whereas the theoretical calculation results are much lower than the verified and other experimental values. The results in our present work decline with the increase of neutron energy around 14 MeV. At the neutron energies of 13.5 MeV and 14.1 MeV, our results are consistent, within experimental error,with those of the excitation curve of Mannhart and Schmidt [21] and Yuan et al.[23] at the same energy as well as the evaluated values of JEFF-3.3 at the corresponding energy. At 14.1 MeV neutron energy, our result is consistent, within experimental error, with that of the verified values of CENDL-3.1. At 14.4 MeV neutron energy, our result is between that of the verified values of JEFF-3.3,CENDL-3.1, and ENDF/B-VIII.0, and the theoretical calculation result. At 14.8 MeV neutron energy, our result is consistent, within experimental error, with the theoretical calculation results.

The ^{46}Ti(n,p)$^{46m+g}$Sc reaction cross-sections are shown in Table 3 and Fig.5. They show that the trends of these excitation curves of JEFF-3.3, CENDL-3.1, ENDF/B-VIII.0 and the results calculated through the computer code Talys-1.9 decrease with increasing neutron energy around 14 MeV, however the extent of their reduction is different. In addition, the theoretical calculation results are much lower than these evaluated values and all experimental values. At the neutron energies 13.5, 14.1, and 14.4 MeV, our results are consistent, within experimental error, with those of the excitation curve of Ikeda et al. [17]. At the neutron energies of 13.5 MeV and 14.1 MeV, our results are consistent, within experimental error, with those of the evaluated values of JEFF-3.3 at the corresponding energies, whereas at 14.1 MeV neutron energy,

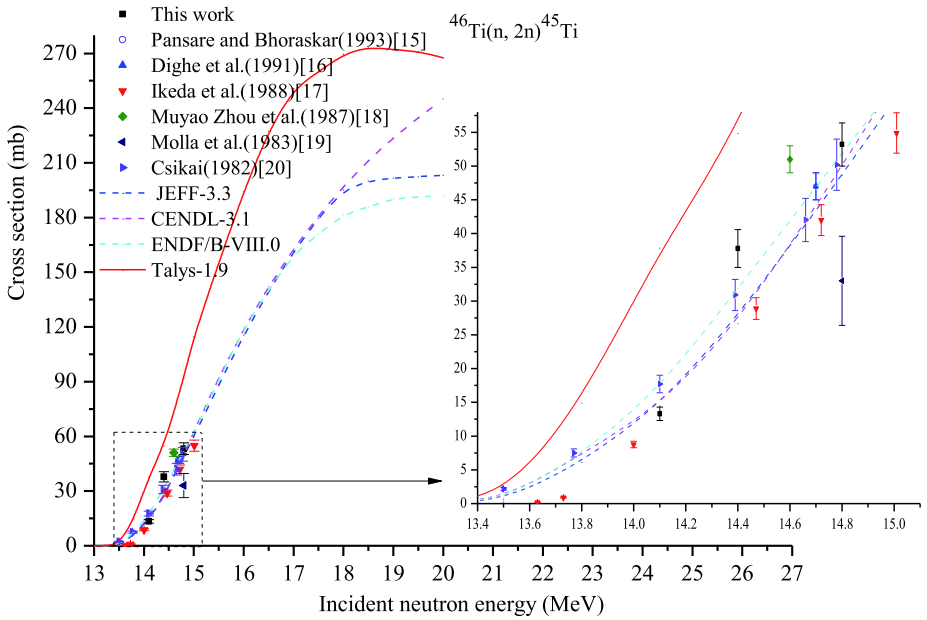

Fig. 3. (color onlie) Cross-section of ^{46}Ti(n,2n)^{45}Ti reaction.

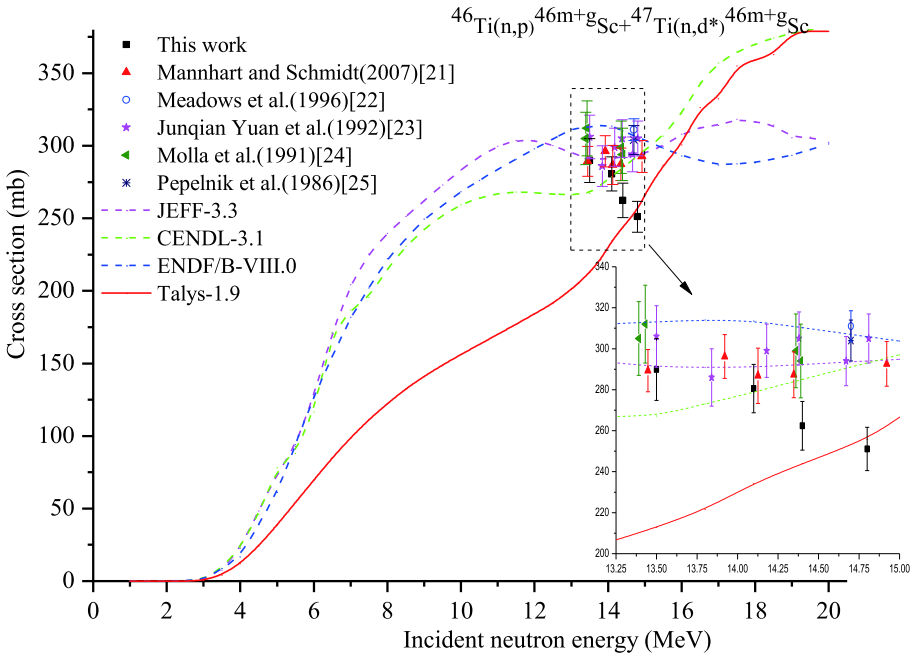

Fig. 4. (color online) Cross-section of ^{46}Ti(n,p)$^{46m+g}$Sc + ^{47}Ti(n,d*)$^{46m+g}$Sc reaction.

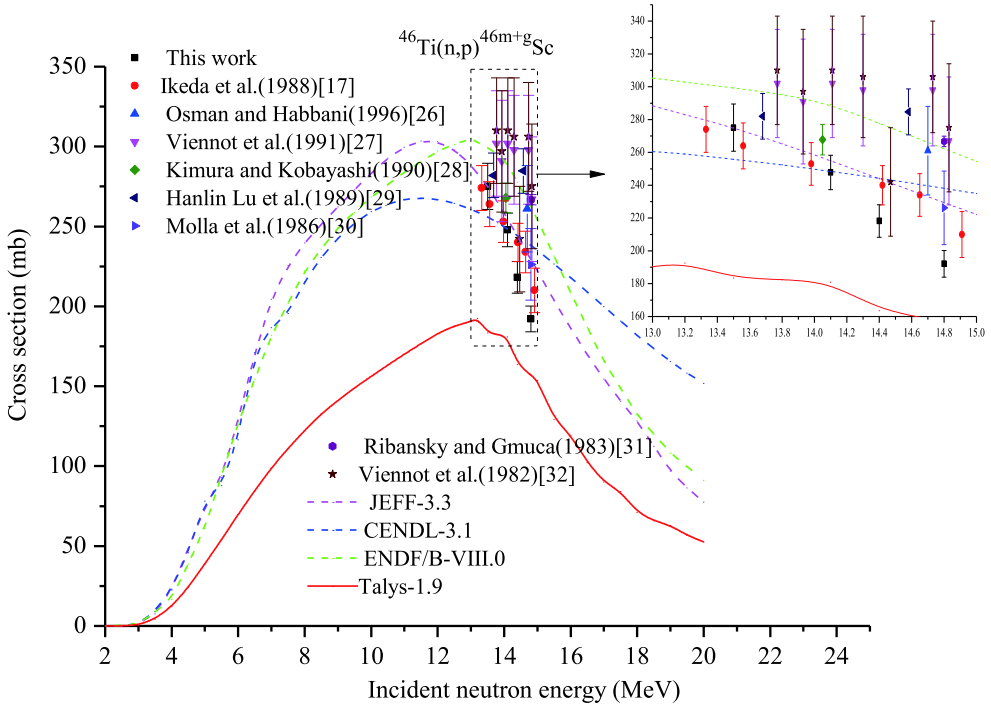

Fig. 5. (color online) Cross-section of ^{46}Ti(n,p)$^{46m+g}$Sc reaction.

our results agree, within experimental error, with the verified value of CENDL-3.1. At neutron energies of 14.4 MeV and 14.8 MeV, our results are between those of the evaluated values of JEFF-3.3, CENDL-3.1, and ENDF/B-VIII.0 and the theoretical calculation results.

For the ^{47}Ti(n,p)^{47}Sc + ^{48}Ti(n,d*)^{47}Sc reaction, which can be seen from Table 4 and Fig.6, the trends of these excitation curves of JEFF-3.3, CENDL-3.1, ENDF/B-VIII.0, and the results calculated by Talys-1.9 are decreasing with increasing neutron energy around 14 MeV, however the extent of their reduction is different. In addition, the theoretical calculation results are much higher than these verified values. Whereas the cross-sections of Mannhart and Schmidt [21] , Viennot et al. [34], and our results increase with the increasing neutron energy around 14 MeV. At the neutron energies of 13.5, 14.1,

14.4, and 14.8 MeV, our results, within experimental error, are consistent with those of the excitation curve of Mannhart and Schmidt [21]. At the neutron energies of 14.1 MeV and 14.8 MeV, our results, within experimental error, are consistent with those of the excitation curve of Viennot et al.[34] at the same energy.

For the ^{47}Ti(n,p)^{47}Sc reaction, which can be seen from Table 4 and Fig.7, there are small discrepancies in the verified values of JEFF-3.3, CENDL-3.1 and ENDF/B-VIII.0 around 14 MeV neutron energy, whereas the results calculated by Talys-1.9 are much higher than the verified and all experimental values. At the neutron energies of 13.5, 14.1, and 14.8 MeV, our results are in agreement, within experimental error, with those of the excitation curve of Ikeda et al. [17] as well as the evaluated values of ENDF/B-VIII.0 at the corresponding energy.

For the ^{48}Ti(n,p)^{48}Sc + ^{49}Ti(n,d*)^{48}Sc reaction, which can be seen from Table 5 and Fig.8, the trends of these excitation curves of JEFF-3.3, CENDL-3.1, ENDF/B-VIII.0, and the results calculated by Talys-1.9 are increasing with increasing neutron energy around 14 MeV. In addition, the theoretical calculation results are much higher than these verified and all experimental values. At the neutron energies of 13.5, 14.1, and 14.4 MeV, our

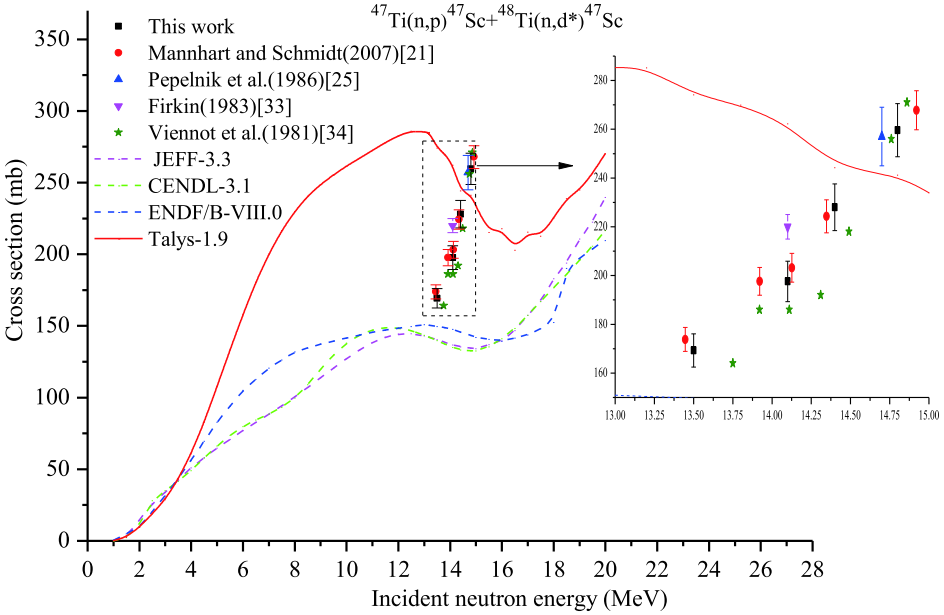

Fig. 6. (color online) Cross-section of ^{47}Ti(n,p)^{47}Sc + ^{48}Ti(n,d*)^{47}Sc reaction.

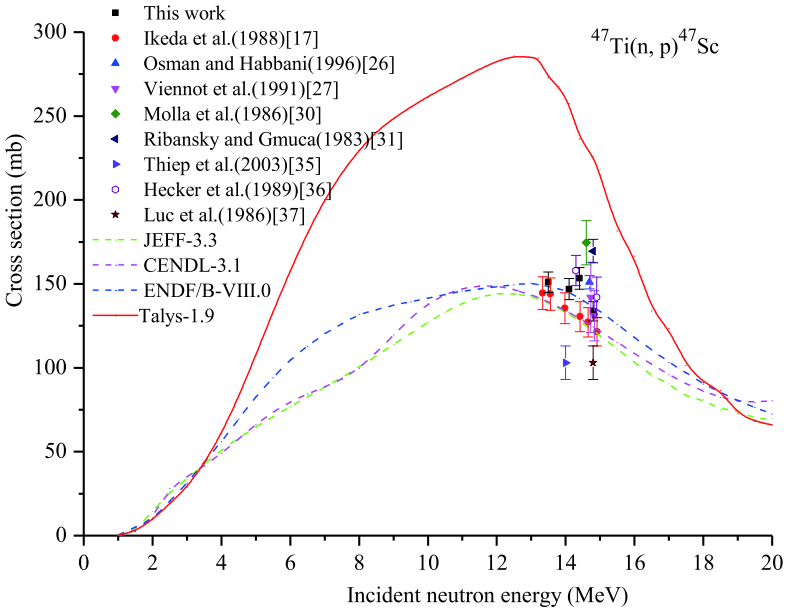

Fig. 7. (color online) Cross-section of ^{47}Ti(n,p)^{47}Sc reaction.

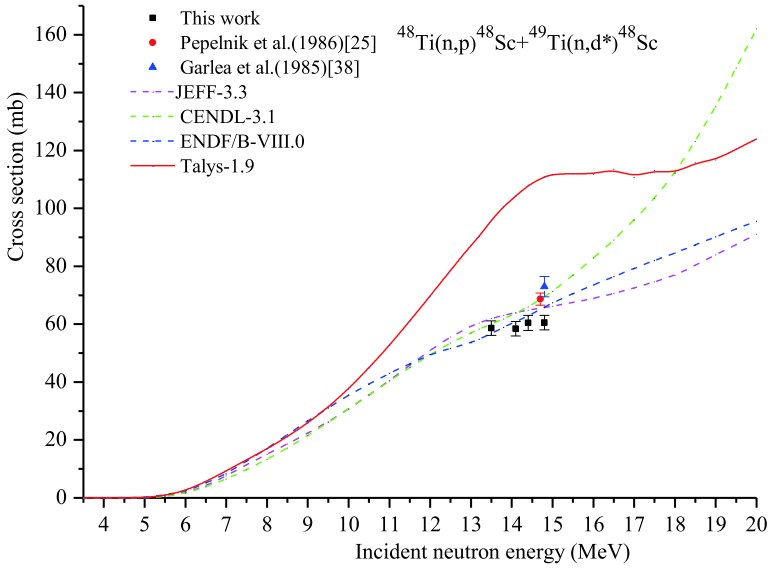

Fig. 8. (color online) Cross-section of ^{48}Ti(n,p)^{48}Sc + ^{49}Ti(n,d*)^{48}Sc reaction.

results, within experimental error, are consistent with the evaluated values of ENDF/B-VIII.0 at the corresponding energies, whereas at 13.5 MeV neutron energy, our results agree, within experimental error, with the obtained value of CENDL-3.1.

For the ^{48}Ti(n,p)^{48}Sc reaction, we can see from Table 5 and Fig.9 that these excitation curves of JEFF-3.3, CENDL-3.1, ENDF/B-VIII.0, and the results calculated by Talys-1.9 exhibit an inflection point, which stems from the change in trend from increasing to decreasing with increasing neutron energy in the neutron energy range of 13–16 MeV. In addition, the theoretical calculation results are much higher than these verified values, and the experimental data that contain our experimental values. At neutron energies of 13.5, 14.1, 14.4, and 14.8 MeV, our results, within experimental error, are consistent with those of the excitation curve of Ikeda et al. [17] and Lu et al. [29] at the same energies, as well as the verified values of CENDL-3.1 and ENDF/B-VIII.0 at the corresponding energies. At 13.5 MeV neutron energy, our result agrees, within experimental error, with that of Yuan et al. [23]. At 14.8 MeV neutron energy, our result is, within experimental error, consistent with those of Luc et al. [37] and Gupta et al. [41], whereas at the neutron energies of 14.4 MeV and 14.8 MeV, our results are in agreement, within experimental error, with the evaluated values of JEFF-3.3 at the corresponding energies.

For the ^{50}Ti(n,α)^{47}Ca reaction, we can see from Table 6 and Fig.10 that the trends of these excitation curves of JEFF-3.3, CENDL-3.1, ENDF/B-VIII.0, and the results by Talys-1.9 are increasing with increasing neutron energy around 14 MeV, however the extent of their increase is different. In addition, the theoretical calculation results are much lower than these evaluated values and all experimental values. At the neutron energies of 13.5, 14.1, 14.4, and 14.8 MeV, our results, within experimental error, agree very well with those of the excitation curve of Yuan et al. [23] and Subasi et al. [42] at the same energies, as well as with the verified values of ENDF/B-VIII.0 at the corresponding energies. At neutron energies of 14.1, 14.4, and 14.8 MeV, our results, within experimental error, are consistent with the obtined values of CENDL-3.1 at the corresponding energies.

In summary, although there are discrepancies between our results and those of earlier experimental data taken from the literature, due to differences in experimental methods, equipments, datum processing methods, and the nuclear parameters used, in general our results in the vicinity of neutron energy of 14 MeV agree with some previous experimental values as well as some verified data of JEFF-3.3, CENDL-3.1, and ENDF/B-VIII.0. For the ^{46}Ti(n,2n)^{45}Ti, ^{47}Ti(n,p)^{47}Sc + ^{48}Ti(n,d*)^{47}Sc, ^{47}Ti(n,p)^{47}Sc, ^{48}Ti(n,p)^{48}Sc + ^{49}Ti(n,d*)^{48}Sc, and ^{48}Ti(n,p)^{48}Sc reactions, the calculated results by Talys-1.9 code with default parameters are much higher than the experimental results and the verified data, whereas for the ^{46}Ti(n,p)$^{46m+g}$Sc + ^{47}Ti(n,d*)$^{46m+g}$Sc, ^{46}Ti(n,p)$^{46m+g}$Sc, and ^{50}Ti(n,α)^{47}Ca reactions, the calculated results by the Talys-1.9 code with default parameters are much lower than the experimental results and the verified data. This means that the theoretically calculated model (Talys-1.9 code) with default parameters is not suitable for the calculation of nuclear reaction cross-sections on titanium isotopes around the neutron energy of 14 MeV. For the ^{46}Ti(n,p)$^{46m+g}$Sc + ^{47}Ti(n,d*)$^{46m+g}$Sc reaction, the trends of these excitation curves of JEFF-3.3, CENDL-3.1, and ENDF/B-VIII.0 are different around the neutron energy of 14 MeV. For the ^{47}Ti(n,p)^{47}Sc + ^{48}Ti(n,d*)^{47}Sc reaction, the trends of these excitation curves of JEFF-3.3, CENDL-3.1, and ENDF/B-VIII.0 are decreasing with increasing neutron

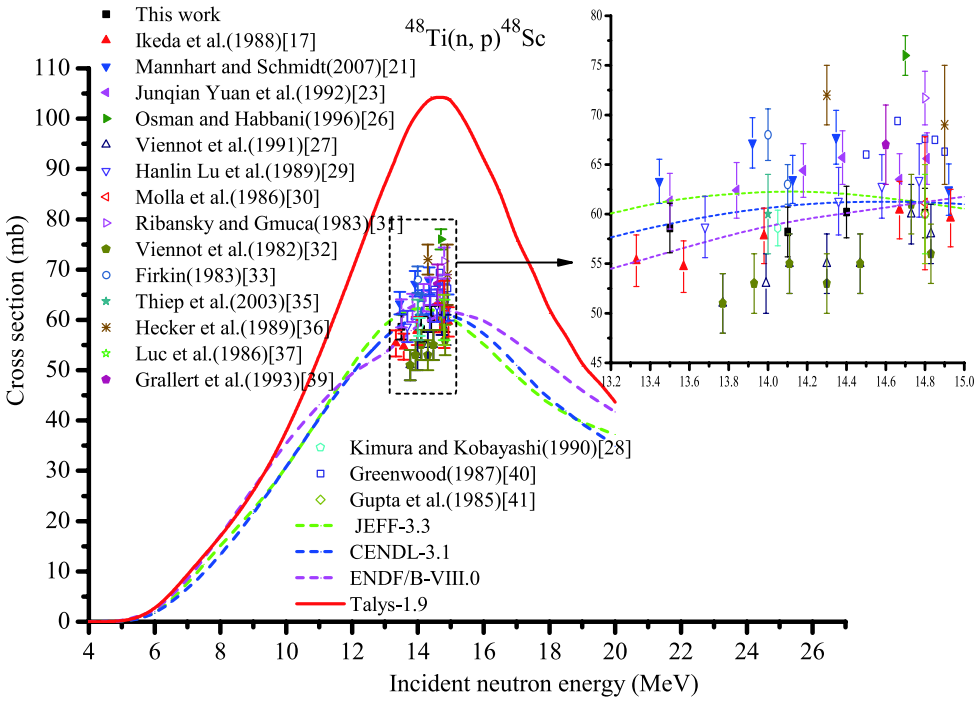

Fig. 9. (color online) Cross-section of ^{48}Ti(n,p)^{48}Sc reaction.

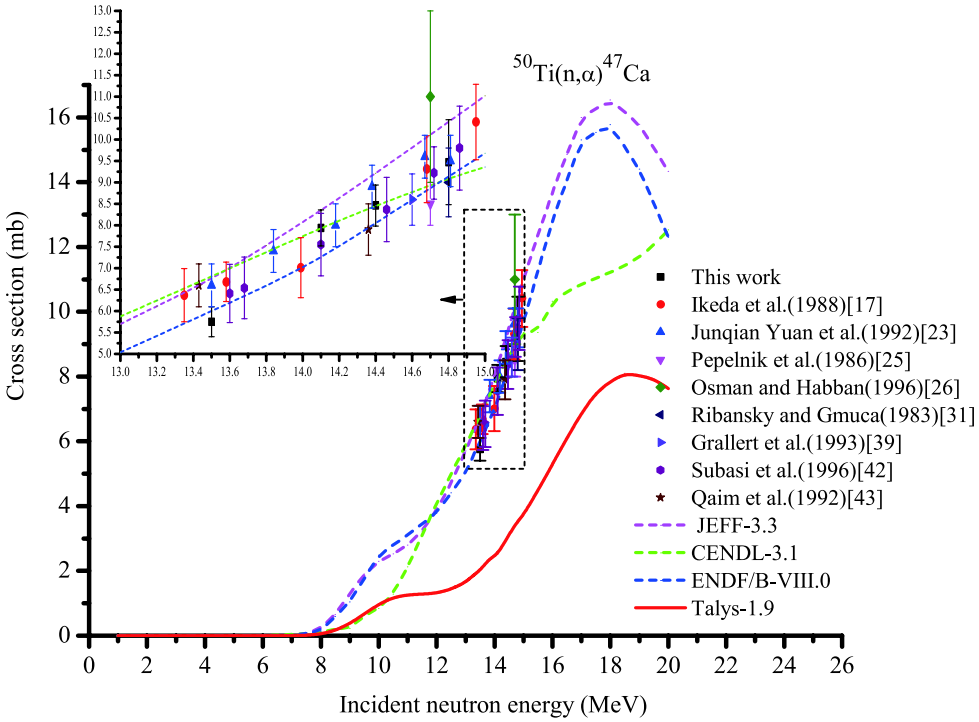

Fig. 10. (color online) Cross-section of ^{50}Ti(n,α)^{47}Ca reaction.

energy around 14 MeV, whereas the experimental cross-section data increase with increasing neutron energy around 14 MeV. This means that new excitation curves for the ^{46}Ti(n,p)$^{46m+g}$Sc+^{47}Ti(n,d*)$^{46m+g}$Sc and ^{47}Ti(n,p)^{47}Sc+^{48}Ti(n,d*)^{47}Sc reactions around the neutron energy of 14 MeV need to be specified.

4 Conclusion

In this study, the experimental cross-sections for the ^{46}Ti(n,2n)^{45}Ti, ^{46}Ti(n,p)$^{46m+g}$Sc+^{47}Ti(n,d*)$^{46m+g}$Sc, ^{46}Ti(n,p)$^{46m+g}$Sc, ^{47}Ti(n,p)^{47}Sc+^{48}Ti(n,d*)^{47}Sc, ^{47}Ti(n,p)^{47}Sc, ^{48}Ti(n,p)^{48}Sc + ^{49}Ti(n,d*)^{48}Sc, ^{48}Ti(n,p)^{48}Sc, and ^{50}Ti(n,α)^{47}Ca re-

actions were measured around the neutron energy of 14 MeV using the activation technique. In general, our results around the neutron energy of 14 MeV agree with some previous experimental values as well as some verified data of JEFF-3.3, CENDL-3.1, and ENDF/B-VIII.0.

The theoretically calculated model (Talys-1.9 code) with default parameters is not suitable for the calculation of nuclear reaction cross-sections on titanium isotopes around the neutron energy of 14 MeV. To calculate nuclear reaction cross-sections on titanium isotopes around the neutron energy of 14 MeV, it is necessary to adjust the relevant parameters of the Talys-1.9 code according to reliable experimental data.

The new results measured in this work are useful for strengthening the database and are expected to aid in new evaluations of some cross-sections of titanium isotopes around the neutron energy of 14 MeV.

We would like to thank the crew of the K-400 Neutron Generator at the Institute of Nuclear Physics and Chemistry China Academy of Engineering Physics for performing the irradiation studies.

References

1 Experimental Nuclear Reaction Data (EXFOR), Database Version of June 29, 2018, IAEA Nuclear Data Services. <https://www-nds.iaea.org/>
2 M. M. Rahman, S. M. Qaim, Nucl. Phys. A, **435**: 43 (1985)
3 M. Bostan, S. M. Qaim, Phys. Rev. C, **49**: 266 (1994)
4 F. Cserpak, S. Sudar, J. Csikai et al, Phys. Rev. C, **49**: 1525 (1994)
5 C. D. Nesaraja, S. Sudár, and S. M. Qaim, Phys. Rev. C, **68**: 024603 (2003)
6 V.E. Lewis and K.J. Zieba, Nucl. Instrum. Methods, **174**: 141 (1980)
7 NuDat 2.7, IAEA Nuclear Data Services. <http://www.nndc.bnl.gov/nudat2/>
8 R.B.Firestone, V.S.Shirley, Table of Isotopes.Wiley, New York (1996)
9 Xiangzhong Kong, Rong Wang, Yongchang Wang et al, Appl. Radiat. Isot., **50**: 361 (1999)
10 M. Wagner, H. Vonach, A. Pavlik et al, Phys. Daten Phys. Data, **13-5**: 183 (1990)
11 A.Koning, S. Hilaire, and S. Goriely, User Manual of Talys-1.9, 2017, http://www.talys.eu/download-talys/
12 A. J. Koning and D. Rochman, Nucl Data Sheets, **113**: 2841-2934 (2012)
13 A. J. Koning and J. P. Delaroche, Nucl Phys A, **713**: 231-310 (2003)
14 J. Raynal, Notes on ECIS94, CEA Saclay Report No. CEAN-2772, 1994
15 G. R. Pansare and V. N. Bhoraskar, Int. Journal of Modern Physics E, **2**: 259 (1993)
16 P. M. Dighe, F. R. Pansare, Ranjita Sarkar et al, Indian Journal of Pure and Applied Physics, **29**: 665 (1991)
17 Y. Ikeda, C. Konno, K. Oishi et al, Rept: JAERI Reports, No. 1312 (1988), Japan
18 Muyao Zhou, Yongfa Zhang, Chuanshan Wang et al, Chinese J. of Nuclear Physics, **9**: (1987)
19 N. I. Molla, M. Mizanul Islam, M. Mizanur Rahman et al, Bangladesh report to the I.N.D.C., No.002 (1983), Austria
20 J. Csikai, Conf: Conf.on Nucl.Data for Sci. and Technol. 414 (1982), Belgium
21 W. Mannhart, D. Schmidt, Rept: Phys. Techn. Bundesanst. No.53 (2007), Germany
22 J. W. Meadows, D. L. Smith, L. R. Greenwood et al, Annals of Nuclear Energy, **23**: 877 (1996)
23 Junqian Yuan, Yongchang Wang, Xiangzhong Kong et al, High Energy Physics and Nucl. Physics., **16**: 57 (1992)
24 N. I. Molla, S. M. Qaim, H. Liskien et al, Applied Radiation and Isotopes, **42**: 337 (1991)
25 R. Pepelnik, B. Anders, B. M. Bahal et al, Rept: Ges. Kernen.-Verwertung, Schiffbau and Schiffahrt, No.86-E-29 (1986), Germany
26 K. T.Osman, F. I. Habbani, Rept: Sudanese report to the I.N.D.C., No.001 (1996), Austria
27 M. Viennot, M. Berrada, G. Paic et al, Nuclear Science and Engineering, **108**: 289 (1991)
28 I. Kimura, K. Kobayashi, Nuclear Science and Engineering, **106**: 332 (1990)
29 Hanlin Lu, Dahai Wang, Yijun Xiaet al, Rept: Chinese report to the I.N.D.C., No.16 (1989), Austria
30 N. I. Molla, M. M. Rahman, S. Khatun et al, Rept: Bangladesh report to the I.N.D.C., No.003 (1986), Austria
31 I. Ribansky, S. Gmuca, Jour. of Physics G, **9**: 1537 (1983)
32 M. Viennot, A. Ait Haddou, A. Chiadli et al, Conf: Conf. on Nucl. Data for Sci. and Technol., 406 (1982), Belgium
33 S. Firkin, Rept: A.E.R.E. Harwell Reports, No.3350 (1983), UK
34 M. Viennot, A. Chiadli, G. Paic et al, Annual Report, No.4 (1981), Morocco
35 T. D. Thiep, N. V. Do, T. T. An et al, Nuclear Physics, Section A, **722**: 568 (2003)
36 W. V. Hecker, J. R. Williams, W. L. Alford et al, Sect.B, **40/41**: 478 (1989)
37 H. D. Luc, P. N. Ngoc, N. V. Do et al, Vietnam report to the I.N.D.C., No.5 (1986), Austria
38 I. Garlea, C. Garlea, D. Dobrea et al, Revue Roumaine de Physique, **30**: 673 (1985)
39 A. Grallert, J. Csikai, Cs. M. Buczko et al, Rept: IAEA Nucl.Data Section report to the I.N.D.C., No.286 (1993), Austria
40 L. R. Greenwood, Conf: American Soc. of Testing and Materials Reports, No.956 (1987), USA
41 J. P. Gupta, H. D. Bhardwaj, and R. Prasad, Pramana, **24**: 637 (1985)
42 M. Subasi, M. Bostan, M. N. Erduran et al, Nuclear Science and Engineering, **122**: 423 (1996)
43 S. M. Qaim, M. Uhl, N. I. Molla et al, Physical Review. C, **46**: 1398 (1992)
44 Fengqun Zhou, Lei Gao, Xiangzhong Kong et al, Phys. Rev. C, **80**: 054615 (2009)